J Elast (2009) 96: 81–95
DOI 10.1007/s10659-009-9199-z

A Pressurized Functionally Graded Hollow Cylinder with Arbitrarily Varying Material Properties

Xian-Fang Li · Xu-Long Peng

Received: 16 October 2008 / Published online: 8 April 2009

Abstract The elastic analysis of a pressurized functionally graded material (FGM) annulus or tube is made in this paper. Different from existing studies, this study deals with an axisymmetrical FGM hollow cylinder or disk with arbitrarily varying material properties. A simple and efficient approach is suggested, which reduces the associated problem to solving a Fredholm integral equation. The resulting equation is approximately solved by expanding the solution as series of Legendre polynomials. The stresses and displacements can be represented in terms of the solution to the equation. For radius-dependent Young's modulus, numerical results of the distribution of the radial and circumferential stresses are presented graphically. Our results indicate that change in the gradient of the FGM tube does not produce a substantial variation of the radial stress, but strongly affects the distribution of the hoop stress. In particular, the hoop stress may reach its maximum at an internal position or at the outer surface when the tube is internally pressurized. The results obtained are helpful in designing FGM cylindrical vessels to prevent failure.

Keywords Functionally graded materials · Pressurized cylindrical tube · Arbitrarily varying gradients

Mathematics Subject Classification (2000) 74E05 · 74B05 · 45B05

1 Introduction

Thin annuli or sufficient long circular tubes are a class of typical structures such as turbine motors, flywheels, delivery pipes, etc. which have been widely used in aerospace, marine, and civil engineering applications. For a homogeneous hollow annular disk or tube, the elastic behavior of this class of structures subjected to external pressure is well-known [1]. By material tailoring, a hollow multi-layered cylinder made of homogenous isotropic materials

X.-F. Li (✉) · X.-L. Peng
IMST, School of Civil Engineering and Architecture, Central South University, Changsha 410083, China
e-mail: xfli@mail.csu.edu.cn

can be optimized for their special purposes. However, this still gives rise to the discontinuity of the hoop stress and mismatch of strain across the interface. Such a jump in the hoop stress can be obviated for a functionally graded material (FGM) hollow cylinder with continuously varying material properties [2], which may lower the occurrence of failure of an internally pressurized tube, in particular in high temperature environment. Due to this reason, FGM tubes have attracted considerable attention in recent years [3–10].

The analysis of stresses in a cylindrically inhomogeneous anisotropic elastic tube and bar subjected to pressure, shearing, torsion and extension have been made in [11–13]. Tarn and Chang [14] analyzed torsion of cylindrically orthotropic elastic circular bars with radial inhomogeneity by considering the end effects. In previous studies on FGM hollow cylinders, the Young's modulus of the cylindrical tube is often assumed to obey a special law, while Poisson's ratio is an unchanged constant. For example, a radial inhomogeneity assumption of power-law form is frequently adopted in [6, 15–18], etc. For the case where Young's modulus is dominated by $E_0 r^\beta$ (r being the radial coordinate of the cylinder), an exact closed-form solution has been derived for a pressurized hollow cylinder in [16, 19], respectively. More recently, for other cases with constant Poisson's ratio and varying Young's modulus including $E(r) = Ar + B$ (A and B being material constants), $E(r) = E_0 e^{\beta r}$ (E_0 and β being material constants), the elastic behaviors of a hollow cylindrical pressure vessel have been studied by using special functions and series expansion in [2, 18, 20, 21]. A cylinder with an exponentially varying elastic modulus along the radial coordinate and a constant Poisson's ratio has also been analyzed with application of the Michell stress function in [22]. A more general form of elastic modulus varying along the radial direction has been considered and explicit expressions for the radial and hoop stresses in terms of relevant special functions have been obtained in [23].

Most of the above-mentioned works are focused on a specific gradient variation, and the boundary value problem associated with a hollow annulus or tube may be solved by special techniques. For a hollow cylindrical pressure vessel with Young's modulus and Poisson's ratio of arbitrarily varying gradient, it is much desirable to develop a sufficiently general method for solving such problems. For this purpose, a novel analytical approach is presented in this paper to solve the elastic problem of FGM cylindrical pressure vessels. The material properties of the cylinders may arbitrarily vary, in a continuous or piecewise-constant manner, corresponding to FGM or multilayered hollow cylinders, respectively. The associated elastic problem is reduced to a Fredholm integral equation. By approximately solving the resulting equation, the distribution of the radial and circumferential stresses can be determined. As an example, an internally pressurized cylindrical vessel is analyzed, and numerical results are presented graphically to show the effects of gradient on the radial and circumferential stresses. The circumferential stress exhibits a completely different response from that of a homogeneous tube. In particular, the maximum hoop stress may occur at an interior point or at the outer surface.

2 Theoretical Formulation

Consider a hollow annular disk or an infinitely long hollow circular cylinder having uniform thickness $b - a$, a and b being the inner and outer radii of the hollow annulus, respectively. The hollow disk or cylinder is assumed to be subjected to axisymmetric loading, so that the problem under consideration is axisymmetric. Let us suppose that the hollow disk or cylinder is made of an isotropic, linearly elastic material. Along the radius direction, Young's

modulus and Poisson's ratio are assumed to vary in an arbitrary manner, i.e.,

$$E = E(r), \qquad \nu = \nu(r), \quad a \le r \le b. \tag{1}$$

If $E(r)$ and $\nu(r)$ are continuous, and this case corresponds to so-called FGM hollow disks or cylinders, while if $E(r)$ and $\nu(r)$ are piecewise-constant functions, this case gives perfectly-bonded multilayered hollow disks or cylinders with each layer having individual constant Young's modulus and Poisson's ratio. The following derivation is suitable for not only continuous $E(r)$ and $\nu(r)$ but also discontinuous $E(r)$ and $\nu(r)$, so the approach given in this paper is unified.

For such an inhomogeneous hollow disk or cylinder, of much interest are the axisymmetric radial and hoop stresses σ_r and σ_θ dependent on r. They satisfy the following equilibrium equation [1]:

$$\frac{d\sigma_r}{dr} + \frac{\sigma_r - \sigma_\theta}{r} = 0, \tag{2}$$

where the body force has been neglected.

To obtain the distribution of σ_r and σ_θ, we express them in terms of a single radial displacement component u_r by the constitutive equations of a linearly elastic material:

$$\sigma_r = \frac{E(r)}{1-\nu^2(r)}\left[\varepsilon_r + \nu(r)\varepsilon_\theta\right], \tag{3}$$

$$\sigma_\theta = \frac{E(r)}{1-\nu^2(r)}\left[\varepsilon_\theta + \nu(r)\varepsilon_r\right], \tag{4}$$

with

$$\varepsilon_r = \frac{du_r}{dr}, \qquad \varepsilon_\theta = \frac{u_r}{r}. \tag{5}$$

It is worth noting that the above constitutive equations are valid for a hollow disk in a state of plane stress. For a similar inhomogeneous hollow cylinder in a state of plane strain, it is sufficient to replace $E(r)$ and $\nu(r)$ with $E(r)/[1-\nu^2(r)]$ and $\nu(r)/[1-\nu(r)]$ respectively. For simplicity, the present derivation is based on the constitutive equations of plane stress state, and the results to be obtained only apply to a hollow annular disk. For an infinitely long hollow cylinder in plane strain state, the corresponding results are readily given from those for plane stress state only with a straightforward substitution.

Usually, the material properties $E(r)$ and $\nu(r)$ are assumed to take specified functions including exponential and power-law forms. A goal of such assumptions is to exactly get the distribution of stresses by means of special techniques for solving ordinary differential equations. In the following study, no restriction on the material properties is needed. This is completely different from the previous analyses. We start with rewriting (3) as

$$\frac{du_r}{dr} + \frac{\nu(r)}{r}u_r = \frac{1-\nu^2(r)}{E(r)}\sigma_r, \tag{6}$$

where (5) has been used. Now, the above equation can be understood as a first-order differential equation for u_r. By solving the above equation, we easily find the solution to be

$$u_r = \frac{1}{\chi(r)}\left[A + \int_a^r \frac{[1-\nu^2(s)]\chi(s)}{E(s)}\sigma_r(s)ds\right], \tag{7}$$

where A is a constant to be determined through appropriate boundary conditions, and $\chi(r)$ is a known function, defined by

$$\chi(r) = \exp\left[\int_a^r \frac{\nu(s)}{s} ds\right]. \tag{8}$$

On the other hand, eliminating ε_r from (3) and (4) and after collections we get

$$\sigma_\theta = \nu(r)\sigma_r + \frac{E(r)}{r} u_r. \tag{9}$$

From (7) and (9), we make some observations. Once the radial stress component σ_r is determined, the radial displacement component can be evaluated through (7), then the hoop stress component σ_θ can be obtained by (9). In particular, the radial displacement component u_r is always continuous, even for discontinuous or piecewise continuous material properties $E(r)$ and $\nu(r)$, as expected. The reason is that the integrals involved in (7) and (8) are continuous, regardless of the fact that the integrand is continuous or piecewise continuous function. However, for perfectly-bonded multilayered hollow disks or cylinders, from (9) σ_θ is seen to have a jump at each interface due to discontinuous material properties $E(r)$ and $\nu(r)$ when across each interface. Such a jump in σ_θ at each interface disappears if hollow disks or cylinders are made of FGM materials with continuously varying material properties. This advantage prevents FGM hollow disks or cylinders from delamination and cracking at distinct interfaces owing to stress concentration or abrupt jump at the interfaces.

Next, putting (7) into (9), then into (2), after some algebra we get an integro-differential equation as follows:

$$\frac{d\sigma_r}{dr} + \frac{1-\nu(r)}{r}\sigma_r - \frac{E(r)}{r^2\chi(r)}\left[A + \int_a^r \frac{[1-\nu^2(\rho)]\chi(\rho)}{E(\rho)}\sigma_r(\rho)d\rho\right] = 0. \tag{10}$$

Furthermore, by integrating both sides of the above equation with respect to r, one can get

$$\sigma_r + \int_a^r K(r,\rho)\sigma_r(\rho)d\rho = B + Af(r), \tag{11}$$

where

$$\begin{aligned} K(r,\rho) &= \frac{1-\nu(\rho)}{\rho} - \frac{[1-\nu^2(\rho)]\chi(\rho)}{E(\rho)}\int_\rho^r \frac{E(s)}{s^2\chi(s)}ds, \\ f(r) &= \int_a^r \frac{E(s)}{s^2\chi(s)}ds. \end{aligned} \tag{12}$$

Note that $K(r,\rho)$ and $f(r)$ in (11) are known, depending on varying Young's modulus and Poisson's ratio, A and B are two unknown constants, which can be determined by using proper conditions associated to the inner and outer surfaces.

3 Solution Procedure

In this section, we consider two typical cases and give the corresponding stress distribution. For other cases, solution procedure is similar and omitted here. In what follows, the following two cases are particularly concerned.

- Case A: the hollow cylinder is subjected to uniform pressure, q_i and q_o, at the inner and outer surfaces, respectively. The corresponding boundary conditions can be stated as

$$\sigma_r(a) = q_i, \qquad \sigma_r(b) = q_o. \tag{13}$$

- Case B: the hollow cylinder is subjected to uniform pressure, q_i, at the inner surface, and displacement of the outer surface is given. The corresponding boundary conditions can be stated as

$$\sigma_r(a) = q_i, \qquad u_r(b) = u_o. \tag{14}$$

For case A, using two boundary conditions in (13), we can obtain two algebraic equations from (11), from which unknown constants A and B can be determined as follow:

$$\begin{aligned} A &= \frac{q_o - q_i}{f(b)} + \frac{1}{f(b)} \int_a^b K(b,\rho)\sigma_r(\rho)d\rho, \\ B &= q_i. \end{aligned} \tag{15}$$

Now inserting the above results back into (11) and after rearrangement, we get a Fredholm integral equation for the radial stress component σ_r

$$\sigma_r + \int_a^b L^A(r,\rho)\sigma_r(\rho)d\rho = h^A(r), \tag{16}$$

where

$$\begin{aligned} h^A(r) &= q_i + \frac{f(r)}{f(b)}(q_o - q_i), \\ L^A(r,\rho) &= \begin{cases} K(r,\rho) - \frac{f(r)}{f(b)}K(b,\rho), & \rho < r, \\ -\frac{f(r)}{f(b)}K(b,\rho), & \rho > r. \end{cases} \end{aligned} \tag{17}$$

For case B, from the first boundary condition at the inner surface in (14) it is easy to find $B = q_i$. To determine another unknown constant A, we apply the second boundary condition in (14) to (7) and get

$$A = u_o\chi(b) - \int_a^b \frac{[1-\nu^2(s)]\chi(s)}{E(s)}\sigma_r(s)ds. \tag{18}$$

Next, we substitute the above result as well as $B = q_i$ into (11), leading to the following Fredholm integral equation:

$$\sigma_r + \int_a^b L^B(r,\rho)\sigma_r(\rho)d\rho = h^B(r), \tag{19}$$

where

$$\begin{aligned} h^B(r) &= q_i + u_o\chi(b)f(r), \\ L^B(r,\rho) &= \begin{cases} \frac{1-\nu(\rho)}{\rho} + \frac{[1-\nu^2(\rho)]\chi(\rho)}{E(\rho)}f(\rho), & \rho < r, \\ \frac{[1-\nu^2(\rho)]\chi(\rho)}{E(\rho)}f(r), & \rho > r. \end{cases} \end{aligned} \tag{20}$$

As a consequence, the final equations for two cases in question are both Fredholm integral equations, and for later convenience of analysis we introduce normalized variables x and t such that

$$r = \frac{b+a}{2} + \frac{b-a}{2}x, \qquad \rho = \frac{b+a}{2} + \frac{b-a}{2}t. \tag{21}$$

Then (16) and (19) can be rewritten as a unified normalized form

$$\sigma(x) + \int_{-1}^{1} \bar{L}(x,t)\sigma(t)dt = g(x), \tag{22}$$

where

$$\sigma(x) = \sigma_r(r), \qquad g(x) = h^J(r), \qquad \bar{L}(x,t) = \frac{b-a}{2}L^J(r,\rho), \quad J = A, B. \tag{23}$$

To obtain a desired distribution of $\sigma(x)$, it is sufficient to seek the solution of (22). Since it is a Fredholm integral equation, many existing techniques may be invoked to determine the numerical or approximate solution to (22). In what follows we employ the expansion method [24] and expand the solution as series of orthogonal polynomials. The convergence of this approach can be found in [24]. Here Legendre polynomials are chosen. If neglecting sufficiently small error, the unknown $\sigma(x)$ can be approximately expanded as:

$$\sigma(x) = \sum_{n=0}^{N} c_n P_n(x), \quad -1 \le x \le 1, \tag{24}$$

where $P_n(x)$ are Legendre polynomials and c_n are unknown coefficients. Here the first $N+1$ terms are chosen and the rest are disregarded owing to negligible error. To determine c_n, inserting (24) into (22) leads to

$$\sum_{n=0}^{N} c_n P_n(x) + \sum_{n=0}^{N} c_n \int_{-1}^{1} \bar{L}(x,t)P_n(t)dt = g(x). \tag{25}$$

With the help of the orthogonality property of Legendre polynomials over $[-1, 1]$, i.e.

$$\int_{-1}^{1} P_m(x)P_n(x)dx = \frac{2}{2m+1}\delta_{mn}, \tag{26}$$

where δ_{mn} denotes the Kronecker delta symbol, $m, n = 1, 2, \ldots$, we multiply both sides of (25) by $P_m(x)$ and then integrate from -1 to 1 with respect to x, yielding a system of linear algebraic equations:

$$\frac{2}{2m+1}c_m + \sum_{n=0}^{N} l_{mn}c_n = g_m, \quad m = 0, 1, 2, \ldots, N \tag{27}$$

with

$$l_{mn} = \int_{-1}^{1}\int_{-1}^{1} P_m(x)\bar{L}(x,t)P_n(t)dtdx, \tag{28}$$

$$g_m = \int_{-1}^{1} P_m(x)g(x)dx. \tag{29}$$

Once $c_m (m = 0, 1, \ldots, N)$ are determined from the above system, the distribution of the radial stress component $\sigma_r(r) = \sigma(x)$ can be evaluated from (24). Furthermore, the unknown constant A can be given and so the radial displacement u_r and the distribution of the circumferential stress component σ_θ may be calculated from (7) and (9), respectively.

4 Numerical Results and Discussions

In this section, numerical computations are carried out for arbitrarily varying Young's modulus and Poisson's ratio. First, prior to the presentation of the numerical results of an FGM disk or cylinder with arbitrary gradient, let us examine the effectiveness and accuracy of the present method. This can be done for the case where Young's modulus and Poisson's ratio are given by

$$E(r) = E_o \left(\frac{r}{b}\right)^{\beta}, \quad \nu(r) = \nu, \tag{30}$$

where E_o is the Young's modulus at the outer surface. For this specially varying Young's modulus, when the inner surface is compressed by uniform pressure $-p$ and the outer surface is traction free, the exact stress distribution is

$$\sigma_r(r) = -p \left(\frac{a}{r}\right)^{(2+k-\beta)/2} \frac{b^k - r^k}{b^k - a^k}, \tag{31}$$

$$\sigma_\theta(r) = p \left(\frac{a}{r}\right)^{(2+k-\beta)/2} \frac{1}{b^k - a^k} \left[\frac{2-(\beta+k)\nu}{\beta+k-2\nu} b^k - \frac{2-(\beta-k)\nu}{\beta-k-2\nu} r^k\right], \tag{32}$$

for case A [16, 19]. For case B, we have

$$\sigma_r(r) = -p \left(\frac{a}{r}\right)^{(2+k-\beta)/2} \frac{(\beta+k-2\nu)b^k - (\beta-k-2\nu)r^k}{(\beta+k-2\nu)b^k - (\beta-k-2\nu)a^k}, \tag{33}$$

$$\sigma_\theta(r) = p \left(\frac{a}{r}\right)^{(2+k-\beta)/2} \frac{[2-(\beta+k)\nu]b^k - [2-(\beta-k)\nu]r^k}{(\beta+k-2\nu)b^k - (\beta-k-2\nu)a^k}, \tag{34}$$

where the outer surface is subjected to zero displacement and

$$k = \sqrt{\beta^2 + 4 - 4\beta\nu}. \tag{35}$$

In order to show the convergence of the solution, we calculate the numerical results by choosing $N = 2, 4, 8$ in (24) and compare them in plane stress state with the exact ones for case A given by (31) and (32). Theoretical analysis of convergence can be found in [24]. Here we only list the corresponding absolute errors, $|\sigma^{\text{calculated}} - \sigma^{\text{exact}}|$, at three special positions (the inner and outer surfaces, and the middle position $r = (a+b)/2$) in Tables 1 and 2 for the radial and hoop stresses, respectively, where $\beta = 2$ and $\nu = 0.3$. From Tables 1 and 2, it is seen that the series solution for $a/b = 0.8$ converges faster than that for $a/b = 0.1$, which is because that σ_r and σ_θ exhibit singular behavior when r tends to zero, as seen from (31) and (32). In particular, for $a/b = 0.8$, the series solution when taking $N = 2$ gives quite accurate and stable results, whereas for $a/b = 0.1$ we need take larger N values, which causes it to achieve high accuracy. From Tables 1 and 2, when taking $N = 8$, the numerical results are very close to the exact ones and therefore, in the following calculations, we choose $N = 8$ in (24).

Table 1 Absolute error of the radial stress for case A when $\beta = 2$, $\nu = 0.3$

N	$a/b = 0.1$			$a/b = 0.8$		
	Inner	Middle	Outer	Inner	Middle	Outer
2	0.30366	0.03583	0.09869	0.00165	5.8072E–05	0.00154
4	0.10913	8.54102E–03	0.03492	5.76959E–05	3.34159E–07	5.45166E–05
8	0.01089	6.40184E–04	0.00369	2.47362E–04	1.33414E–06	1.74900E–05

Table 2 Absolute error of the hoop stress for case A when $\beta = 2$, $\nu = 0.3$

N	$a/b = 0.1$			$a/b = 0.8$		
	Inner	Middle	Outer	Inner	Middle	Outer
2	0.06508	0.00279	0.03212	4.92797E–04	6.16486E–06	4.6467E–04
4	0.02965	6.77078E–04	0.01074	1.96943E–05	3.46174E–06	2.02387E–05
8	0.00326	1.11061E–04	0.00113	7.65941E–05	3.90341E–06	9.13088E–06

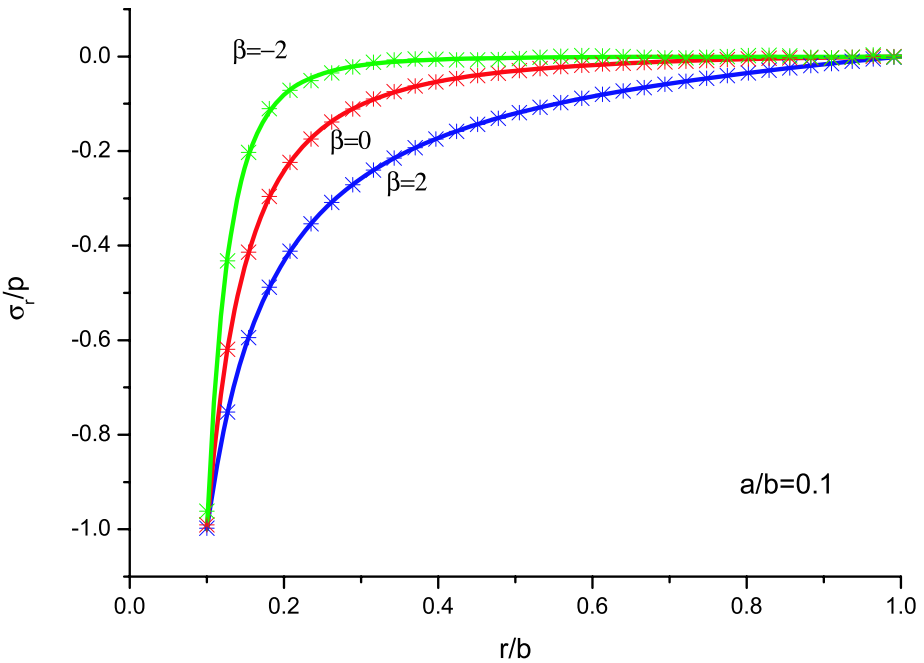

Fig. 1 A comparison of the exact and numerical results of the radial stress component $\sigma_r(r)/p$ in an FGM hollow disk with $p_o = 0$, $p_i = -p$, $\nu = 0.3$ and $a/b = 0.1$, where Young's modulus is given by (30); *solid lines*: exact results, *scattered data*: numerical results

Using the present method, numerical results are obtained for several different values of β, and presented graphically for the radial and circumferential stress components of an FGM hollow disk with the ratio of $a/b = 0.1$ and $\nu = 0.3$ for case A in Figs. 1 and 2, respectively. For comparison, we also plot the corresponding curves according to the above-mentioned exact solutions. From Figs. 1 and 2, it is readily seen that the method suggested in the present paper is very efficient for an FGM disk or cylinder.

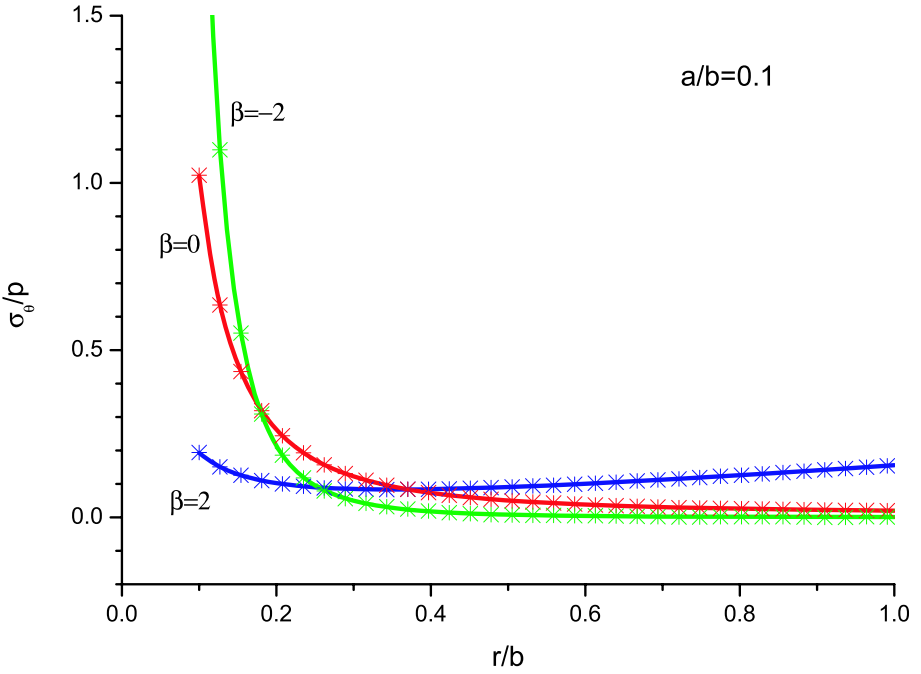

Fig. 2 A comparison of the exact and numerical results of the circumferential stress component $\sigma_\theta(r)/p$ in an FGM hollow disk with $p_o = 0$, $p_i = -p$, $\nu = 0.3$ and $a/b = 0.1$, where Young's modulus is given by (30), *solid lines*: exact results, *scattered data*: numerical results

Next, we consider Young's modulus obeying the relation:

$$E(r) = E_i + (E_o - E_i)\,\frac{r^\beta - a^\beta}{b^\beta - a^\beta}, \tag{36}$$

where E_i and E_o are Young's moduli at the inner and outer surfaces, respectively. For simplicity we still assume an unchanged constant Poisson's ratio since Poisson's ratio of most materials varies slightly. It is worth mentioning that a variable Poisson's ratio along the radius direction does not give rise to any difficulty in determining the solution of the problem. For this reason, the results of the radial and hoop stress components for an FGM tube with $\nu = 0.3$ are presented for $E_o/E_i = 0.1, 10$ in Figs. 3 and 4, respectively. From Figs. 3 and 4, the radial stress is compressive and monotonically increases from $-p$ at the inner surface to zero at the outer surface. Moreover, the distribution of $\sigma_r(r)$ is similar, regardless of $E_o/E_i = 0.1, 10$. Compared to $\sigma_r(r)$, the effects of E_o/E_i on the distribution of $\sigma_\theta(r)$ are marked. In the FGM tube, $\sigma_\theta(r)$ is tensile, which is about $0.4p$ when $E_o/E_i = 10$, and about $1.18p$ when $E_o/E_i = 0.1$ at the inner surface, meaning that $\sigma_\theta(r) < |\sigma_r(r)|$ possibly occurs. This is to say that the onset of failure may be caused by the radial stress for an FGM tube. This important observation was also made in [16] for the model (30). Note that for a homogeneous hollow tube, $\sigma_\theta(r) > |\sigma_r(r)|$ is always true [1]. In addition, $\sigma_\theta(r)$ is also observed to be continuous, which is a substantial difference from that for a layered tube. For the latter case, a discontinuous $\sigma_\theta(r)$ can be derived, which can be expected from (9) owing to mismatch of Young's modulus.

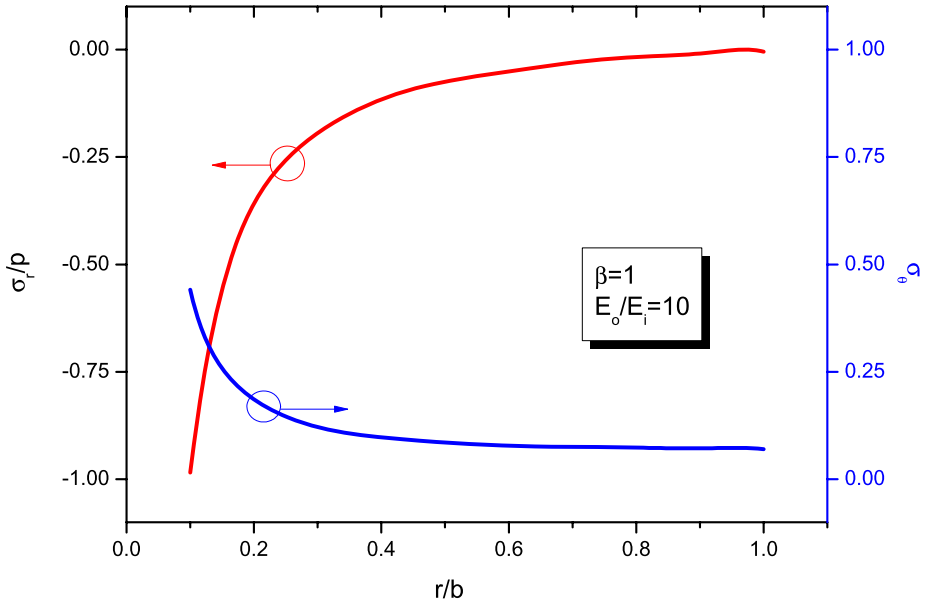

Fig. 3 The distribution of the stress components in an internally pressurized FGM tube with $p_i = -p$, $\nu = 0.3$ and $a/b = 0.1$, where Young's modulus is governed by (36) with $E_o/E_i = 10$, $\beta = 1$

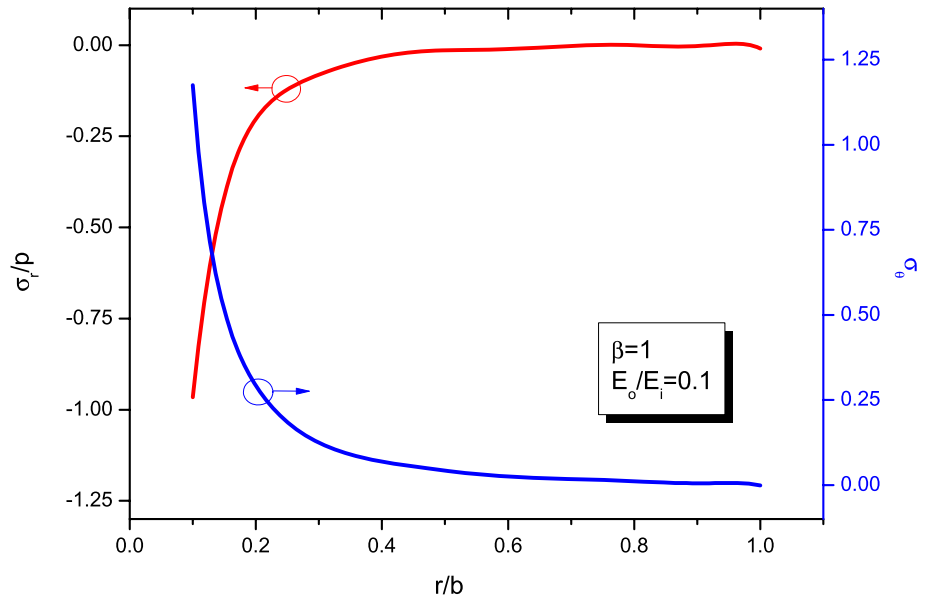

Fig. 4 The distribution of the stress components in an internally pressurized FGM tube with $p_i = -p$, $\nu = 0.3$ and $a/b = 0.1$, where Young's modulus is governed by (36) with $E_o/E_i = 0.1$, $\beta = 1$

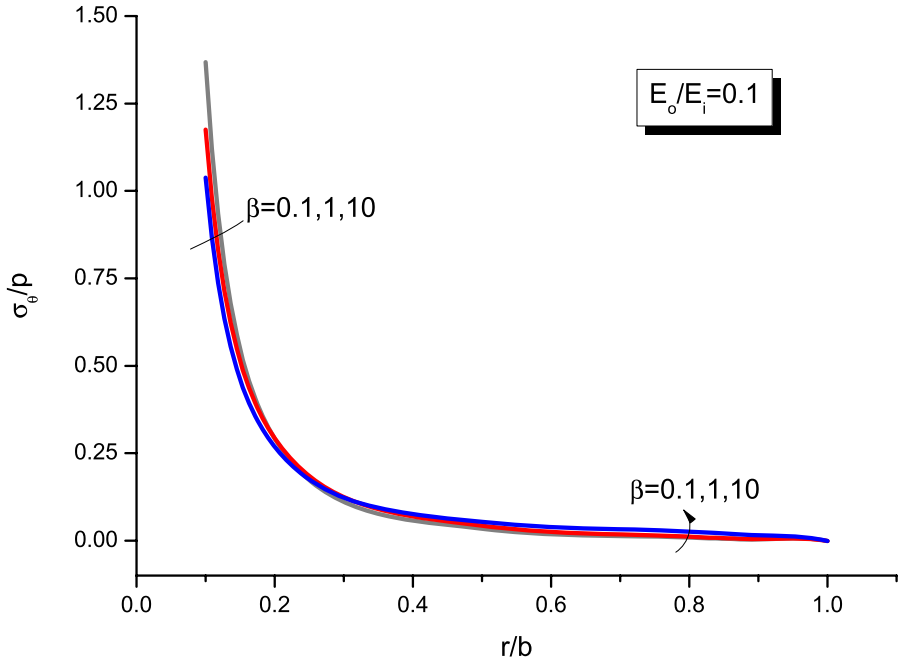

a

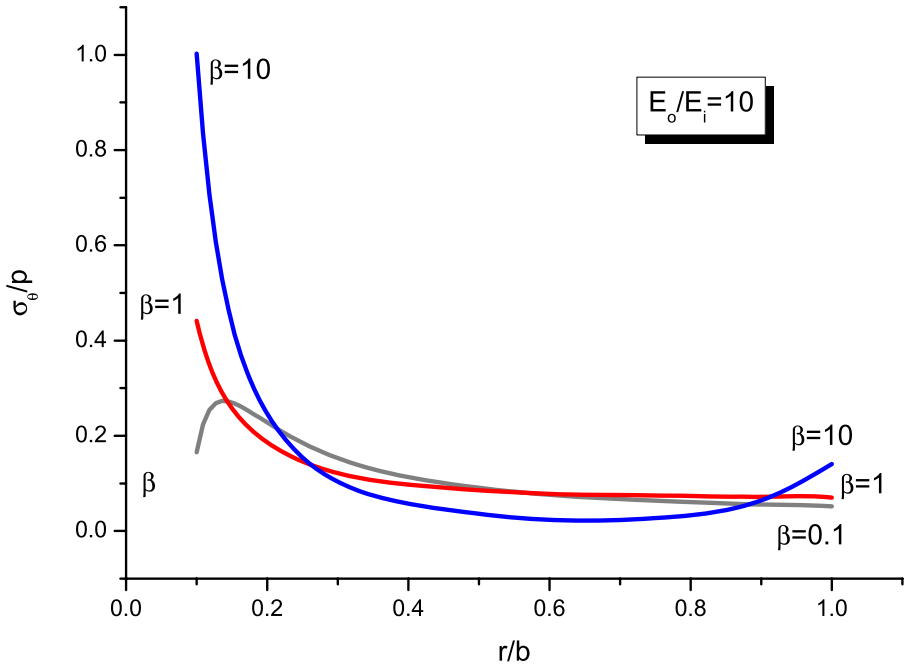

b

Fig. 5 The effects of the gradient index on the variation of the circumferential stress component $\sigma_\theta(r)/p$ against r/b in an internally pressurized FGM tube with $p_i = -p$, $\nu = 0.3$ and $a/b = 0.1$, where Young's modulus is governed by (36) with (**a**) $E_o/E_i = 0.1$, (**b**) $E_o/E_i = 10$

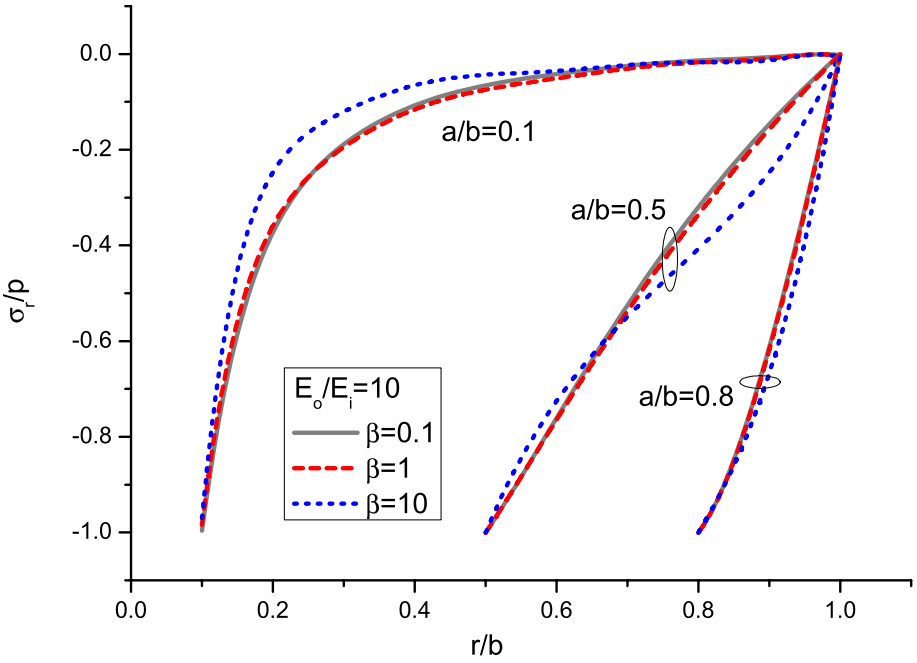

Fig. 6 The distribution of the radial stress component $\sigma_r(r)/p$ in an internally pressurized FGM tube with various tube thicknesses and $p_i = -p$, $\nu = 0.3$, where Young's modulus is governed by (36) with $E_o/E_i = 10$

Figures 5a, b are devoted to the effects of the gradient index β on the distribution of the circumferential stress for $E_o/E_i = 0.1, 10$, respectively. As seen from Fig. 5a, $\sigma_\theta(r)$ monotonically decreases with distance from the inner surface for $E_o/E_i = 0.1$. Such behavior was first shown in [16] for Young's modulus governed by (30). However, the trend of $\sigma_\theta(r)$ for $E_o/E_i = 10$ in Fig. 5b is completely different from that observed in Fig. 5a. In particular, $\sigma_\theta(r)$ has a minimum value at an internal position rather than at the surfaces for $\beta = 10$. Such a characteristic also occurs for Young's modulus governed by (30) [16]. In contrast, $\sigma_\theta(r)$ has a maximum value at an internal position for $\beta = 0.1$. This feature seems to be new. Moreover, the difference between the maximum and minimum values of $\sigma_\theta(r)$ in this case is least. This result is useful for designing an FGM tube to prevent from failure since the maximum $\sigma_\theta(r)$ value is dramatically lowered, and moreover, there is a slight change in the distribution of $\sigma_r(r)$ for different β values, which is displayed in Fig. 6.

The above feature is further examined for various thicknesses $a/b = 0.1, 0.5, 0.8$. For comparison, the distribution of $\sigma_r(r)$ in an FGM tube with $E_o/E_i = 10$ is shown for various gradients in Fig. 6. Clearly, $\sigma_r(r)$ always monotonically increases from $-p$ to zero. The gradient β has a somewhat effect on the distribution of $\sigma_r(r)$. Nevertheless, for $\sigma_\theta(r)$, the gradient β plays a crucial role for a thick FGM tube (Figs. 5b and 7a). For a thin FGM tube, the influence of β becomes insignificant, which can be viewed from Fig. 7b. Note that for this case, $\sigma_\theta(r)$ achieves its maximum at the outer surface, which is completely opposite to that for a homogenous tube subjected to internal pressure. No matter which case, it is expedient to design an FGM tube with small gradient index (β value) when $E_o/E_i > 1$ to prevent from failure.

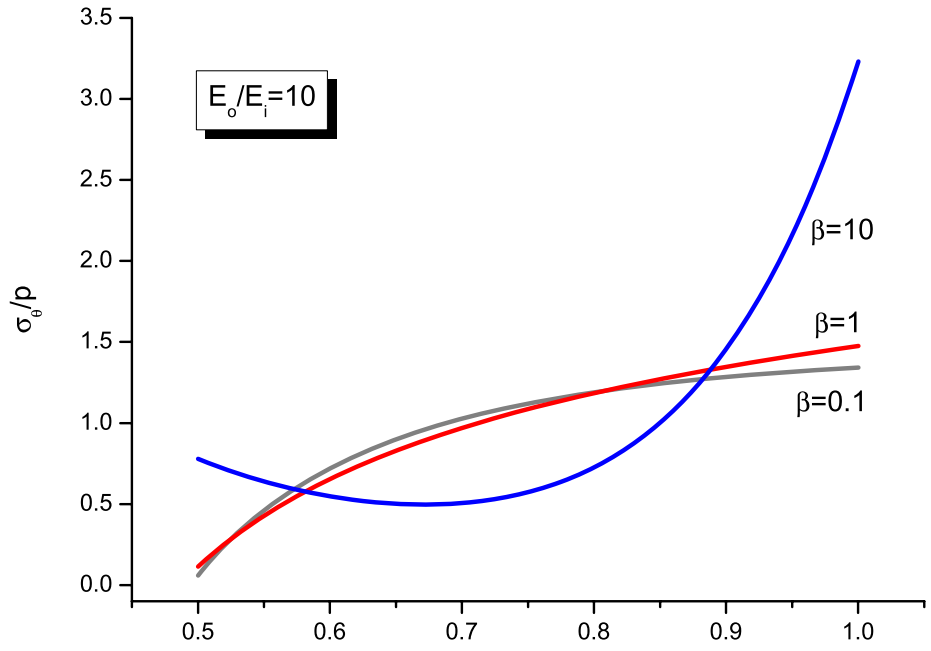

a

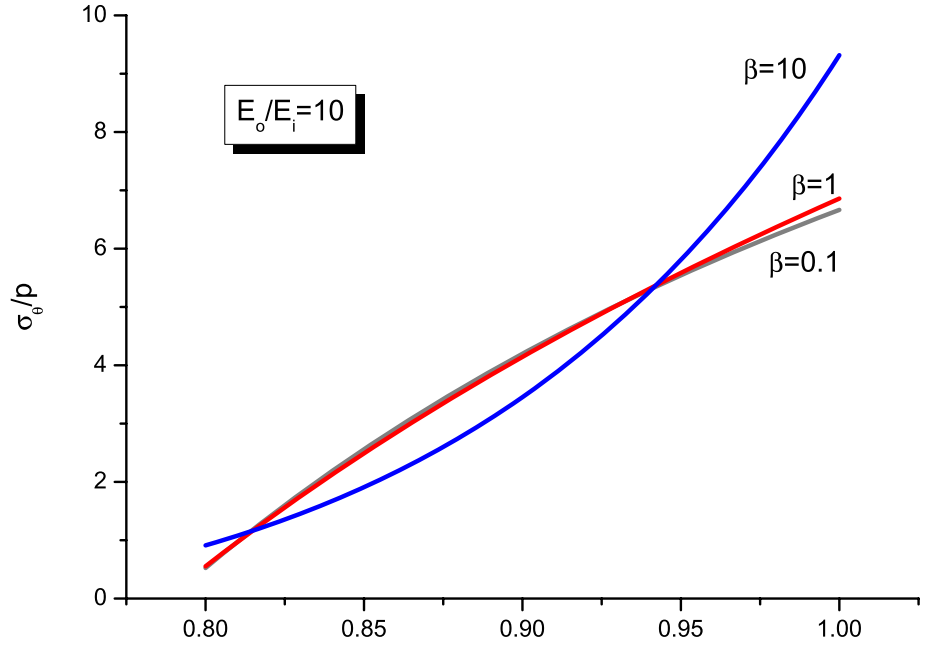

b

Fig. 7 The distribution of the circumferential stress component $\sigma_\theta(r)/p$ in an internally pressurized FGM tube with (**a**) $a/b = 0.5$, (**b**) $a/b = 0.8$ and $p_i = -p$, $\nu = 0.3$, where Young's modulus is governed by (36) with $E_o/E_i = 10$

5 Conclusions

This paper analyzes the elastic behavior of an axisymmetric FGM hollow disk or cylinder. In the previous studies, such a problem is often dealt with for FGM hollow cylinders with some specified gradient variation including exponential and power-law forms, etc. In the present study, the material properties including Young's modulus and Poisson's ratio may be arbitrarily varying functions, in a continuous or discontinuous manner. In addition, the method adopted in this paper is also different. Existing methods are often to solve an ordinary differential equation with variable coefficients via special functions. In contrast, this paper presents a simple and efficient approach for solving this problem. We transform the problem in question to a Fredholm integral equation. Solving the resulting equation, the distribution of the stress components is obtainable. For typically varying material properties, numerical results are evaluated for the radial and circumferential stress distributions and presented graphically. Our results indicate that change in the gradient of the FGM tubes does not produce a substantial variation of the radial stress, but strongly affects the circumferential stress for different tube thicknesses. The obtained results are helpful in designing FGM annuli and tubes for the purpose of structural integrity.

Acknowledgements This work was supported by the National Natural Science Foundation of China under Grant No. 10672189. The authors would like to thank anonymous reviewers for their useful comments for improving the original manuscript.

References

1. Timoshenko, S.P., Goodier, J.N.: Theory of Elasticity, 3rd edn. McGraw-Hill, New York (1970)
2. Shi, Z.F., Zhang, T.T., Xiang, H.J.: Exact solutions of heterogeneous elastic hollow cylinders. Compos. Struct. **79**, 140–147 (2007)
3. Lutz, M.P., Zimmerman, R.W.: Effect of the interphase zone on the bulk modulus of a particular composite. ASME J. Appl. Mech. **63**, 855–861 (1996)
4. Tanaka, K., Watanabe, H., Sugano, Y., Poterasu, V.F.: A multicriterial material tailoring of a hollow cylinder in functionally gradient materials: Scheme to global reduction of thermoelastic stresses. Comput. Methods Appl. Mech. Eng. **135**, 369–380 (1996)
5. Horgan, C.O., Chan, A.M.: The stress response of functionally graded isotropic linearly elastic rotating disks. J. Elasticity **55**, 219–230 (1999)
6. Tarn, J.Q.: Exact solutions for functionally graded anisotropic cylinders subjected to thermal and mechanical loads. Int. J. Solids Struct. **38**, 8189–8206 (2001)
7. Jaabbari, M., Sohrabpour, S., Elsam, M.R.: Mechanical and thermal stresses in a functionally graded hollow cylinder due to radially symmetric loads. Int. J. Press. Vessels Piping **79**, 493–497 (2002)
8. Kim, K.S., Noda, N.: Green's function approach to unsteady thermal stresses in an infinite hollow cylinder of functionally graded material. Acta Mech. **156**, 145–161 (2002)
9. Oral, A., Anlas, G.: Effects of radially varying moduli on stress distribution of nonhomogeneous anisotropic cylindrical bodies. Int. J. Solids Struct. **42**, 5568–5588 (2005)
10. Batra, R.C., Iaccarino, G.L.: Exact solutions for radial deformations of a functionally graded isotropic and incompressible second-order elastic cylinder. Int. J. Non-Linear Mech. **43**, 383–398 (2008)
11. Ting, T.C.T.: Pressuring, shearing, torsion and extension of a circular tube or bar of cylindrically anisotropic material. Proc. R. Soc. Lond. A **452**, 2397–2421 (1996)
12. Ting, T.C.T.: New solutions to pressuring, shearing, torsion and extension of a circular tube or bar. Proc. R. Soc. Lond. A **455**, 3527–3542 (1999)
13. Alshits, V.I., Kirchner, H.O.K.: Cylindrically anisotropic, radially inhomogeneous elastic materials. Proc. R. Soc. Lond. A **457**, 671–693 (2001)
14. Tarn, J.Q., Chang, H.H.: Torsion of cylindrical orthotropic elastic circular bars with radial inhomogeneity: some exact solutions and end effects. Int. J. Solids Struct. **45**, 303–319 (2008)
15. Lekhnitskii, S.G.: Theory of Elasticity of an Anisotropic Body. Mir, Moscow (1981)
16. Horgan, C.O., Chan, A.M.: The pressurized hollow cylinder or disk problem for functionally graded isotropic linearly elastic materials. J. Elasticity **55**, 43–59 (1999)

17. Yang, Y.Y.: Time-dependent stress analysis in functionally graded materials. Int. J. Solids Struct. **37**, 7593–7608 (2000)
18. Theotokoglou, E.E., Stampouloglou, I.H.: The radially nonhomogeneous elastic axisymmetric problem. Int. J. Solids Struct. **45**, 6535–6552 (2008)
19. Tutuncu, N., Ozturk, M.: Exact solutions for stresses in functionally graded pressure vessels. Compos., Part B Eng. **32**, 683–686 (2001)
20. Xiang, H.J., Shi, Z.F., Zhang, T.T.: Elastic analyses of heterogeneous hollow cylinders. Mech. Res. Commun. **33**, 681–691 (2006)
21. Tutuncu, N.: Stresses in thick-walled FGM cylinders with exponentially-varying properties. Eng. Struct. **29**, 2032–2035 (2007)
22. Zhang, X., Hasebe, N.: Elasticity solution for a radially nonhomogeneous hollow circular cylinder. J. Appl. Mech. ASME **66**, 598–606 (1999)
23. Dryden, J., Jayaraman, K.: Effect of inhomogeneity on the stress in pipes. J. Elasticity **83**, 179–189 (2006)
24. Baker, C.T.H.: Expansion methods. In: Delves, L.M., Walsh, J. (eds.) Numerical Solution of Integral Equations, pp. 80–96. Clarendon, Oxford (1974)